
Learning to Optimize for Mixed-Integer Nonlinear Programming

Bo Tang¹ Elias B. Khalil¹ Ján Drgoňa^{2,3}

Abstract

Mixed-integer nonlinear programs (MINLPs) arise in domains as diverse as energy systems and transportation but are notoriously difficult to solve, particularly at scale. While learning-to-optimize (L2O) methods have been successful at continuous optimization, extending them to MINLPs is challenging due to the integer constraints. To overcome this, we propose a novel L2O approach with two integer correction layers to ensure solution integrality and a projection step to improve solution feasibility. Our experiments show that our methods efficiently solve MINLPs with up to tens of thousands of variables, providing high-quality solutions within milliseconds, even for problems where traditional solvers and heuristics fail. This is the first general L2O method for parametric MINLPs, finding solutions to some of the largest instances reported to date.

1. Introduction

Mixed-integer optimization emerges in a broad spectrum of real-world applications involving discrete decisions, such as pricing (Kleinert et al., 2021), battery dispatch (Nazir & Almassalkhi, 2021), transportation (Schouwenaars et al., 2001), and optimal control (Marcucci & Tedrake, 2020). While mixed-integer *linear* programming (MILP) has been widely adopted due to mature exact (Land & Doig, 2010) and heuristic (Crama et al., 2005; Johnson & McGeoch, 1997) solution techniques, many real-world problems involve nonlinear functions, giving rise to mixed-integer nonlinear programs (MINLPs). Unlike MILPs, MINLPs pose greater challenges due to the interplay between discrete variables and non-convex constraints or objectives. While standard methods such as outer approximation (Fletcher & Leyffer, 1994), spatial branch-and-bound (Belotti et al.,

2009), and decomposition techniques (Nowak, 2005) exist, they often struggle to scale to large problems.

Many applications require solving MINLPs within strict time constraints, which imposes additional challenges on traditional optimization methods. To address this, learning-to-optimize (L2O) methods present a promising alternative by leveraging machine learning (ML) to enhance or replace traditional optimization techniques. Among these, *end-to-end optimization* directly maps input problem parameters to solutions using trained models (Kotary et al., 2021b; Chen et al., 2022; Hentenryck, 2025), thus eliminating the need for computationally intensive traditional solvers, offering faster computation and better scalability.

Since many real-world applications typically impose stringent operational, physical, or safety constraints, recent research in machine learning for optimization has focused on the feasibility issue. While various strategies exist, such as embedding hard constraints into neural network architectures (Hendriks et al., 2020), using penalty terms in loss functions for soft constraints (Pathak et al., 2015; Jia et al., 2017), utilizing gauge maps (Li et al., 2022), projecting solutions onto feasible regions (Donti et al., 2021), or domain-specific layers (Chen et al., 2024), these methods are not directly applicable to problems with integer decisions.

This work puts forth the first L2O method for parametric nonlinear optimization problems with mixed-integer decision variables. The challenge of non-differentiability in predicting integer variables has been largely overlooked in L2O methods due to the lack of meaningful gradient information. To address this, we introduce two differentiable correction layers for gradient-based optimization, allowing the neural network to backpropagate with integer outputs. Furthermore, we introduce an efficient gradient-based projection heuristic as a post-processing step, leveraging gradient information through the correction layers to further refine solution feasibility. Our contributions are as follows:

- We develop the first general L2O method for end-to-end learning of solutions to parametric MINLPs.
- We employ a self-supervised learning approach that eliminates the need for labeled data, ensuring scalability and efficiency even for large problem instances.
- We propose computationally efficient learnable correc-

¹Department of Mechanical and Industrial Engineering, University of Toronto, Toronto, ON M5S 1A1, Canada ²Pacific Northwest National Laboratory, Richland, WA 99354, USA ³The Ralph O’Connor Sustainable Energy Institute, Johns Hopkins University, Baltimore, MD 21218, USA. Correspondence to: Ján Drgoňa <jdrgonal@jh.edu>.

tion layers that transform neural network outputs into the integer domain, enabling gradient-based learning for problems with discrete decisions.

- We incorporate a projection step that post-processes an infeasible neural network output by gradient descent towards a feasible integer solution.
- We create and open-source a new parametric MINLP benchmark with tunable problem complexity and scale.
- We validate our method on diverse benchmarks, showcasing its efficiency and high-quality solutions including on some of the largest MINLP instances to date where existing state-of-the-art methods fail.

2. Related Work

End-to-end optimization. These methods aim to train machine learning models to predict the optimization problem solutions, bypassing the need for computationally expensive solvers. One of the earliest approaches was introduced by Hopfield & Tank (1985), who used Hopfield networks to solve the traveling salesperson problem by incorporating a Lagrangian penalty for constraint feasibility. More recently, Fioretto et al. (2020) applied the Lagrangian penalty in the context of continuous non-linear optimization for energy systems. Beyond penalty-based methods, Pan et al. (2020) embedded certain constraints directly into neural networks by leveraging the range of output values and solving linear systems. Although these supervised learning methods significantly reduce inference time, they typically require large offline datasets of pre-solved solutions (Gleixner et al., 2021; Kotary et al., 2021a), which are often computationally too expensive for large-scale problems. This challenge has driven the development of self-supervised learning approaches (Donti et al., 2021), which directly minimize the objective function and constraint violation from predicted values without relying on pre-solved solutions.

Our method is the first to extend this self-supervised end-to-end paradigm to problems involving discrete decision variables, completely removing the need for solvers. This solver-free approach can be efficiently trained at scale, enabling real-time solutions to large-scale MINLP problems.

Constrained neural architectures. For problems that require feasible solutions, effectively handling constraints in neural networks is essential. Specific neural network architectures can be employed to enforce hard constraints. For example, Hendriks et al. (2020) incorporated linear operator constraints into the model design, while Vinyals et al. (2015) and Dai et al. (2017) leveraged the inherent structure of graphs to construct feasible solutions for the traveling salesperson problem. Additionally, Kervadec et al. (2022) demonstrated that using the log-barrier method for inequality constraints can improve accuracy, constraint satis-

faction, and training stability. In contrast to hard constraints, penalty methods (Pathak et al., 2015; Jia et al., 2017), which incorporate inequality constraints through regularization terms in the loss function, have also gained popularity for constraining neural networks. While theoretically weaker, Márquez-Neila et al. (2017) noted that these methods often outperform their hard constraint counterparts in practice. Building on penalty methods, Donti et al. (2021) proposed differentiable correction and completion layers to handle equality and inequality constraints.

To address the challenges of MINLP, we introduce two novel differentiable integer correction layers combined with projection heuristic as a post-processing step, enabling high-quality L2O solutions for mixed-integer problems.

Learning for mixed-integer programming. There has been significant interest in using ML to accelerate the solution of integer programs. The vast majority of the work in this space focuses on learning search strategies for exact MILP solvers. This includes parameter tuning (Xu et al., 2011), preprocessing (Berthold & Hendel, 2021), branching variable selection (Khalil et al., 2016; Alvarez et al., 2017; Gasse et al., 2019; Zarpellon et al., 2021), node selection (He et al., 2014), heuristic selection (Chmiela et al., 2021), and cut selection and generation (Deza & Khalil, 2023; Dragotto et al., 2023). Another line of research relates to learning to heuristically generate solutions for integer linear program (Nair et al., 2020; Khalil et al., 2022; Ding et al., 2020; Sonnerat et al., 2021; Song et al., 2020; Bertsimas & Stellato, 2022; Huang et al., 2023; Ye et al., 2024). We refer to the surveys of Bengio et al. (2021) and Zhang et al. (2023) for more details. In contrast, learning methods for MINLP remain relatively underexplored. Examples include the two-stage algorithm by Cauligi et al. (2021) for efficiently solving mixed-integer convex programs, the supervised learning approach by Baltean-Lugojan et al. (2019) for cut selection in quadratic optimization, a graph neural networks by Nowak et al. (2018) on solving quadratic assignment problems, and a classifier by Bonami et al. (2022) to determine linearization strategies for mixed-integer quadratic problems. The recently proposed SurCO approach by Ferber et al. (2023) is also relevant. They focused on mixed-integer problems with nonlinear objectives, where a linear approximation of the objective simplifies the computation.

Different from all of the above in its scope, our approach focuses on the very general classes of parametric MINLPs.

Differentiable optimization. A different category of methods integrates optimization solvers as layers within deep neural network architectures (Agrawal et al., 2019). These approaches enable gradients of optimization solvers to be computed and propagated during backpropagation, allowing neural networks to handle a variety of opti-

mization problems, such as quadratic programs (Amos & Kolter, 2017; Sambharya et al., 2023), stochastic optimization (Donti et al., 2017), submodular optimization (Djolonga & Krause, 2017), and integer linear programs (Wilder et al., 2019; Berthet et al., 2020; Pogančić et al., 2020). For example, King et al. (2024) demonstrated how differentiable optimization enhances the convergence of proximal operator algorithms by learning proximal metrics in an end-to-end manner. However, as Tang & Khalil (2024) observed, training with differentiable optimizers requires repeatedly solving optimization problems during training, resulting in substantial computational overhead.

In contrast, our self-supervised approach directly generates solutions through neural networks, avoiding iterative solver calls and significantly reducing computational costs.

3. Preliminaries

3.1. Learning Problem Formulation

A generic training formulation for learning-to-optimize with parametric MINLPs is given by:

$$\begin{aligned} \min_{\Theta} \quad & \mathbb{E}[f(\hat{\mathbf{x}}, \boldsymbol{\xi})] \approx \frac{1}{m} \sum_{i=1}^m f(\hat{\mathbf{x}}^i, \boldsymbol{\xi}^i) \\ \text{s.t.} \quad & \mathbf{g}(\hat{\mathbf{x}}^i, \boldsymbol{\xi}^i) \leq 0, \\ & \hat{\mathbf{x}}^i \in \mathbb{R}^{n_r} \times \mathbb{Z}^{n_z}, \quad \hat{\mathbf{x}}^i = \boldsymbol{\psi}_{\Theta}(\boldsymbol{\xi}^i), \quad \forall i \in [m]. \end{aligned}$$

Here, $\boldsymbol{\xi}^i \in \mathbb{R}^{n_{\xi}}$ represents the parameters of training instance i . The neural network $\boldsymbol{\psi}_{\Theta}(\boldsymbol{\xi}^i)$, parameterized by weights Θ , predicts a solution $\hat{\mathbf{x}}^i = (\hat{\mathbf{x}}_r^i, \hat{\mathbf{x}}_z^i)$ for the mixed-integer decision variables, where $\hat{\mathbf{x}}_r^i \in \mathbb{R}^{n_r}$ denotes the continuous part and $\hat{\mathbf{x}}_z^i \in \mathbb{Z}^{n_z}$ denotes the integer part. The objective is to learn the weights Θ that minimize an empirical approximation to the expected objective function while satisfying the inequality constraints $\mathbf{g}(\hat{\mathbf{x}}^i, \boldsymbol{\xi}^i) \leq 0$, where $\mathbf{g}(\cdot)$ is a vector-valued function. We assume that the objective and constraint functions are differentiable.

3.2. Loss Function

Our approach is *self-supervised* because the loss calculation does not rely on labeled data, which is particularly advantageous given the inherent difficulty of computing optimal or feasible solutions to MINLPs. The average value of the objective function $f(\cdot)$ serves as a natural loss function. However, solely minimizing the objective is insufficient when solutions violate the constraints. Therefore, similarly to Donti et al. (2021), we incorporate penalty terms to account for constraint violations. This results in a soft-constrained empirical risk minimization loss, given as:

$$\mathcal{L}(\Theta) = \frac{1}{m} \sum_{i=1}^m \left[f(\hat{\mathbf{x}}^i, \boldsymbol{\xi}^i) + \lambda \cdot \|\mathbf{g}(\hat{\mathbf{x}}^i, \boldsymbol{\xi}^i)_+\|_1 \right], \quad (2)$$

where $\hat{\mathbf{x}}^i = \boldsymbol{\psi}_{\Theta}(\boldsymbol{\xi}^i)$ are the neural network outputs, $\|(\cdot)_+\|_1$ penalizes only positive constraint violations (implemented via a ReLU function), and $\lambda > 0$ is a penalty hyperparameter that balances the trade-off between minimizing the objective function and satisfying the constraints.

3.3. Differentiating through Discrete Operations

Since MINLP involves integer decision variables, neural networks are required to produce discrete outputs. However, these outputs lack gradients, which challenges gradient-based optimization. To address this, we employ the Straight-through Estimator (STE) (Bengio et al., 2013), a widely used method for enabling backpropagation through discrete operations in neural networks. In the forward pass, STE applies a non-differentiable discrete operation, such as rounding down and binarization. In the backward pass, STE substitutes the non-existent gradient of these operations with a smooth approximation. Specifically, STE uses the gradient of the identity function for rounding down, while for binarization, the gradient of the Sigmoid function is applied.

4. Methodology

In this section, we introduce our novel L2O methodology for solving parametric MINLP problems. As illustrated in Figure 1, the approach consists of two core components: integer correction layers and a feasibility projection heuristic.

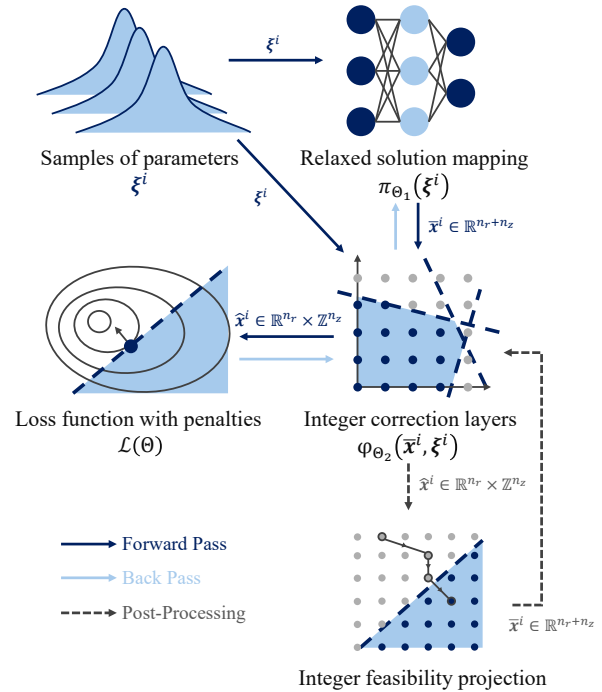


Figure 1: Conceptual diagram for our self-supervised learning-to-optimize approach for parametric MINLP.

4.1. Integer Correction Layers

To handle the integer decision variables in MINLPs, we propose two learnable correction layers: *Rounding Classification* (RC) and *Learnable Threshold* (LT). The mapping $\psi_{\Theta} : \mathbb{R}^{n_{\xi}} \mapsto \mathbb{R}^{n_r} \times \mathbb{Z}^{n_z}$ from an instance parameter vector ξ^i to a mixed-integer solution $\hat{\mathbf{x}}^i$ is performed in two stages:

1. **Relaxed Solution Mapping:** The first step consists in applying a learnable mapping $\pi_{\Theta_1} : \mathbb{R}^{n_{\xi}} \mapsto \mathbb{R}^{n_r+n_z}$, represented by a deep neural network with weights Θ_1 . It outputs a relaxed solution $\bar{\mathbf{x}}^i \in \mathbb{R}^{n_r+n_z}$ without enforcing integrality. Note that continuous variables are also predicted in this first step.
2. **Integer Correction:** The second step is a correction layer $\varphi_{\Theta_2} : \mathbb{R}^{n_r+n_z} \times \mathbb{R}^{n_{\xi}} \mapsto \mathbb{R}^{n_r} \times \mathbb{Z}^{n_z}$ that refines the relaxed solution $\bar{\mathbf{x}}^i$ into a mixed-integer solution. This correction includes a trainable neural network layer δ_{Θ_2} with learnable weights Θ_2 , which takes both the instance parameter vector ξ and the relaxed solution $\bar{\mathbf{x}}^i$ as inputs and learns the rounding behavior for each decision variable.

Algorithm 1 summarizes our proposed approach. Line 1 invokes the first step for solution mapping π_{Θ_1} and lines 2–11 describe both versions of correction φ_{Θ_2} . These layers leverage STE to enable differentiability in handling discrete operations. While STE has been applied in training binarized or quantized neural networks, to the best of our knowledge, this is the first time it has been utilized in the context of learning-to-optimize. Notably, rather than directly applying STE for rounding, we design trainable correction strategies to adaptively guide the rounding process, allowing the correction layer to refine solutions based on instance-specific patterns. As demonstrated in the experimental results, the simplicity of the correction layers is key to fast solution generation in large-scale MINLP problems. Further details on the implementation are provided in Appendix A.

Algorithm 1 Integer Correction Layers: Forward Pass

- 1: **Input:** parameters ξ^i , layers $\pi_{\Theta_1}(\cdot)$ and $\delta_{\Theta_2}(\cdot)$
 - 2: Predict a continuously relaxed solution $\bar{\mathbf{x}}^i \leftarrow \pi_{\Theta_1}(\xi^i)$
 - 3: Obtain an initial correction prediction $\mathbf{h}^i \leftarrow \delta_{\Theta_2}(\bar{\mathbf{x}}^i, \xi^i)$
 - 4: Update continuous variables: $\hat{\mathbf{x}}_r^i \leftarrow \bar{\mathbf{x}}_r^i + \mathbf{h}_r^i$
 - 5: Round integer variables down: $\hat{\mathbf{x}}_z^i \leftarrow \lfloor \bar{\mathbf{x}}_z^i \rfloor$
 - 6: **if** using *Rounding Classification* (RC) **then**
 - 7: Compute rounding direction $\mathbf{b}^i \leftarrow \text{Gumbel-Sigmoid}(\mathbf{h}_z^i)$
 - 8: **else if** using *Learnable Threshold* (LT) **then**
 - 9: Compute thresholds $\mathbf{v}^i \in [0, 1]^{n_z} \leftarrow \text{Sigmoid}(\mathbf{h}_z^i)$
 - 10: Compute rounding direction $\mathbf{b}^i \leftarrow \mathbb{I}((\bar{\mathbf{x}}_z^i - \hat{\mathbf{x}}_z^i) - \mathbf{v}^i > 0)$
 - 11: **end if**
 - 12: Update integer variables: $\hat{\mathbf{x}}_z^i \leftarrow \hat{\mathbf{x}}_z^i + \mathbf{b}^i$
 - 13: **Output:** a mixed-integer solution $\hat{\mathbf{x}}^i$
-

During training, the loss function in Equation (2) is used

to jointly optimize the neural network weights $\Theta = \Theta_1 \cup \Theta_2$, accounting for both the objective function value and constraint violations of the predicted mixed-integer solution $\hat{\mathbf{x}}^i$. Another visualization showing the evolution of solutions over the training process is provided in Appendix B.

RC (line 6) and LT (line 8) differ in how they determine the rounding direction: RC adopts a probabilistic approach to decide the rounding direction for each integer variable, while LT yields a threshold vector to control the rounding process. Both methods are differentiable, easy to train using gradient descent, and computationally efficient during inference. These correction layers can be viewed as an end-to-end learnable extension of the Relaxation Enforced Neighborhood Search (RENS) (Berthold, 2014). Instead of explicitly searching the neighborhood of the relaxed solution, the neural network implicitly learns the corrections required to achieve a feasible integer solution by exploring the solution space near the integer variables while updating the continuous variables.

4.2. Integer Feasibility Projection

Despite the effectiveness of the proposed correction layers in ensuring integer feasibility, penalty-based methods cannot fully guarantee constraint satisfaction, especially in complex instances. To address this, we incorporate a gradient-based projection method as a post-processing step, further improving solution feasibility while maintaining computational efficiency. Unlike conventional projection-based methods that solve an optimization problem, our approach iteratively refines the solution using gradient-based updates that minimize constraint violations $\mathcal{V}(\hat{\mathbf{x}}^i, \xi^i)$. Crucially, because the corrected relaxed solution $\bar{\mathbf{x}}$ is passed through the correction layer $\varphi_{\Theta_2}(\bar{\mathbf{x}}^i, \xi^i)$, the integer domain is naturally restored.

Our approach follows Donti et al. (2021), where feasibility is improved iteratively. However, a key distinction is that we apply this projection only at test time rather than incorporating it into the training process. Training with feasibility projection carries the challenge of retaining computation graphs and computing second-order gradients over multiple projection iterations. Moreover, modifying the network’s outputs during training could interfere with learning dynamics, making optimization less stable.

Algorithm 2 outlines the feasibility projection process, which iteratively refines the relaxed solution $\bar{\mathbf{x}}^i$. This method shares similarities with the feasibility pump (Fischetti et al., 2005): line 4 performs the rounding operation for integrality, while line 9 executes the projection step to minimize constraint violations. By alternating between these two operations, the algorithm effectively achieves feasibility in practice.

The feasibility projection operates on the relaxed solution

Algorithm 2 Integer Feasibility Projection: Inference

```

1: Input: parameters  $\xi^i$ , layers  $\pi_{\Theta_1}(\cdot)$  and  $\varphi_{\Theta_2}(\cdot)$ , step size  $\eta$ 
2: Predict a continuously relaxed solution  $\bar{\mathbf{x}}^i \leftarrow \pi_{\Theta_1}(\xi^i)$ 
3: while True do
4:   Obtain a mixed-integer solution  $\hat{\mathbf{x}}^i \leftarrow \varphi_{\Theta_2}(\bar{\mathbf{x}}^i, \xi^i)$ 
5:   Compute feasibility violation  $\mathcal{V}(\hat{\mathbf{x}}^i, \xi^i) \leftarrow \|\mathbf{g}(\hat{\mathbf{x}}^i, \xi^i)\|_1$ 
6:   if  $\mathcal{V}(\hat{\mathbf{x}}^i, \xi^i) = 0$  then
7:     Break
8:   else
9:     Update relaxed solution  $\bar{\mathbf{x}}^i \leftarrow \bar{\mathbf{x}}^i - \eta \nabla_{\bar{\mathbf{x}}} \mathcal{V}(\hat{\mathbf{x}}^i, \xi^i)$ 
10:  end if
11: end while
12: Output: a mixed-integer solution  $\hat{\mathbf{x}}^i$ 
    
```

$\bar{\mathbf{x}}^i$ rather than the mixed-integer solution $\hat{\mathbf{x}}^i$. This distinction is essential because directly projecting $\hat{\mathbf{x}}^i$ would violate integrality. Instead, since the correction layers preserve differentiability, the relaxed solution $\bar{\mathbf{x}}^i$ can be iteratively updated to reduce constraint violations. The updated $\bar{\mathbf{x}}^i$ is then transformed into a mixed-integer solution via the correction layer φ_{Θ_2} . While heuristic, this projection procedure always successfully produces a final mixed-integer solution adhering to both feasibility and integer constraints.

5. Experimental Results

5.1. Experimental Setup

Methods. Table 1 provides an overview of all the methods used in the following experiments. A 1000-second time limit is enforced for all methods. The experiments evaluate our learning-based methods, Rounding Classification (RC) and Learnable Threshold (LT), against traditional exact optimization (EX), which can compute optimal solutions but is often computationally expensive, and heuristic-based approaches such as Rounding after Relaxation (RR) and root node solutions (N1), which offer faster results without quality guarantees. The enhanced methods, RC-P and LT-P, apply our feasibility projection as a post-processing step on RC and LT to further reduce constraint violations.

Note that baselines EX and N1 include a wide range of heuristics that are embedded in the MINLP solver of choice (Gurobi or SCIP) and that are executed in conjunction with the tree search procedure; we are also implicitly comparing these heuristics, not just to the exact search. As such, the competing methods cover a broad spectrum of optimization strategies, from exact solvers to fast heuristics, allowing for a comprehensive evaluation of solution quality and computational efficiency.

In addition, two ablation studies are conducted to assess the contribution of different components of our correction layers φ_{Θ_2} . These baselines isolate specific aspects of the correction layers to quantify their individual impact on solution quality and constraint satisfaction. Details on the

ablation setup and results are provided in Appendix F.1.

Problem classes. We tested the methods on a variety of optimization problems, including integer quadratic problems, integer non-convex problems, and high-dimensional mixed-integer Rosenbrock problems. These problem classes were selected to cover both convex and non-convex scenarios and evaluate the scalability of the methods in higher-dimensional settings. Each method was assessed in terms of objective value, constraint violation, and solving/inference time, providing a comprehensive view of their performance across different types of problems. Further details on the mathematical formulation and data generation process are provided in Appendix C. The problem classes are as follows:

- **Integer Quadratic Problems (IQPs).** Due to the lack of publicly available datasets for parametric MINLPs, we adapted the benchmark from Donti et al. (2021), originally designed for continuous optimization. We introduced integer constraints and made additional modifications to fit our discrete setting.
- **Integer Non-convex Problems (INPs).** Extending the IQP benchmark, we incorporated a trigonometric term into the objective function, following the approach of Donti et al. (2021). This introduces non-convexity, increasing the complexity of finding optimal solutions. Additionally, we parameterized the constraint matrix to challenge the optimization process further.
- **Mixed-integer Rosenbrock Problems (MIRBs).** This problem is a challenging new benchmark we created to include integer variables, non-linear constraints, tunable problem dimensions, and parametric variations in the objective function and constraints. This problem allows us to evaluate the scalability and the ability to handle complex optimization landscapes, which can represent one of the largest MINLPs to date.

In addition, we evaluated our methods on integer linear programs (MILPs) using the dataset from the MIP Workshop 2023 Computational Competition (Bolusani et al., 2023). These experiments primarily serve to demonstrate that our methods can also handle integer linear cases, though the use of MILP solvers may be preferable. Further details are provided in Appendix F.4.

Training protocol. The solution mapping π_{Θ_1} used across all learning-based methods (RC, LT, and ablation studies) and the neural network δ_{Θ_2} of integer correction for RC and LT are based on fully connected layers with ReLU activations. Further details about the neural network structure and hyperparameters are provided in Appendix D.

For all problems, the training samples 8,000 instances, and the test set includes 100 instances. An additional set of 1,000

Table 1: Summary of Methods. Methods with “*” use a trained model.

Method	Abbr	Description
Rounding Classification*	RC*	Learns to produce probability to classify rounding directions for integer variables.
Learnable Threshold*	LT*	Learns to predict thresholds to guide integer variable rounding.
Exact Solver	EX	Solves problems exactly using Gurobi for the convex and SCIP + Ipopt for the non-convex.
Rounding after Relaxation	RR	Rounds solutions of the continuous relaxation to its nearest integers.
Root Node Solution	N1	Finds the first feasible solution from the root node of the solver, combining various heuristics.

Enhanced Methods: RC-P* and LT-P* that extend RC and LT by incorporating a feasibility projection as post-processing.

instances was used for validation to fine-tune the models and select hyperparameters. Given that our self-supervised approach does not require labels from optimal solutions, it is straightforward to scale up the sample size. For an analysis of the impact of training sample size, refer to Appendix F.3.

Computational setup. Our code is available at <https://github.com/pnnl/L2O-pMINLP>. All experiments were conducted on a system with two Intel Silver 4216 Cascade Lake @ 2.1GHz CPUs, 64GB RAM, and four NVIDIA V100 Volta GPUs. The software environment was configured with Python 3.10.13, PyTorch 2.5.0+cu122 (Paszke et al., 2019) for deep learning models, and NeuroMANCER 1.5.2 (Drgona et al., 2023) for modeling parametric constrained optimization problems.

For exact optimization, Gurobi 11.0.1 (Gurobi Optimization, LLC, 2021) is used as the exact method for integer quadratic problems (IQPs). For those more general mixed-integer non-convex problems, SCIP 9.0.0 (Bestuzheva et al., 2021) was employed, coupled with Ipopt 3.14.14 (Wächter & Biegler, 2006) as the continuous solver. Notably, Gurobi and SCIP are widely recognized as state-of-the-art solvers for MINLP. As highlighted in the comprehensive benchmarking study by Lundell & Kronqvist (2022): “It is clear, however, that the global solvers Antigone, BARON, Couenne and SCIP are the most efficient at finding the correct primal solution when regarding the total time limit. [...] Gurobi also is very efficient when considering that it only supports a little over half of the total number of problems!”

Overall results. As illustrated in Figure 2, exact solvers such as Gurobi and SCIP find better solutions over time but can be somewhat slow. For more complex problem instances, these solvers may fail to find feasible solutions within strict time limits. In contrast, our proposed methods consistently achieve high-quality feasible solutions within milliseconds. To the best of our knowledge, this is the first general approach for efficiently solving MINLPs with up to tens of thousands of variables.

Even when accounting for training time (100 seconds), the overall efficiency of RC and LT remains substantially better.

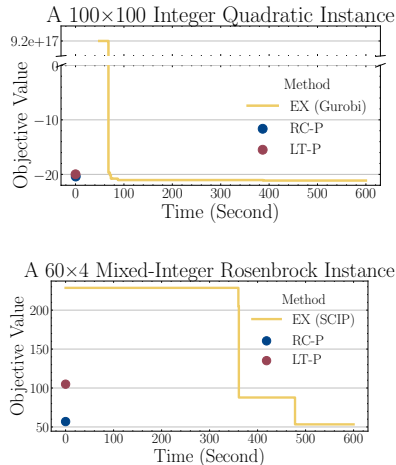


Figure 2: Illustration of objective value evolution for a 100×100 integer Quadratic and 60×4 mixed-integer Rosenbrock problems over 600 seconds. The RC-P and LT-P methods achieve subsecond solutions comparable to those found by exact solvers in hundreds of seconds.

Importantly, once trained, the models effectively generalize to unseen problem instances, making them ideal for repeated problem-solving scenarios where the training cost is amortized (Amos, 2022). Furthermore, RC and LT can generate high-quality initial solutions for exact solvers, reducing the search space and accelerating convergence, thus enhancing the performance of traditional methods.

5.2. Empirical Evaluation

We evaluate our methods on a range of problem instances, including IQPs, INPs, and MIRBs. For IQPs and INPs, we tested problem sizes from 20 decision variables and 20 constraints (20×20) to 1,000 decision variables and 1,000 constraints (1000×1000), while for MIRBs, we experimented with instances ranging from 2 to 20,000 decision variables with the number of constraints fixed at 4. The results are summarized in Table 2, Table 3, and Table 4, corresponding to IQPs, INPs, and MIRBs, respectively. For methods that rely on exact solvers (EX, N1, and RR), the

solver may fail to find any solution within the time limit. To account for this, we report “%Solved”, which indicates the proportion of instances obtained within the given computational budget.

Table 2: Result for IQPs. Each problem size is evaluated on a test set of 100 instances. “Obj Mean” and “Obj Median” represent the mean and median objective values for this minimization problem, with smaller values being better. “% Feasible” denotes the fraction of feasible solutions, and “Time (Sec)” is the average solving/inference time per instance. The “—” symbol indicates that no solution is found for any instance within 1000 seconds.

Method	Metric	20×20	50×50	100×100	200×200	500×500	1000×1000
RC	Obj Mean	-4.237	-12.20	-13.54	-31.62	-73.31	-142.7
	Obj Median	-4.307	-12.20	-13.60	-31.71	-73.38	-142.7
	% Feasible	99%	99%	96%	97%	86%	82%
	Time (Sec)	0.0019	0.0019	0.0022	0.0021	0.0025	0.0042
	Time (Sec)	0.0019	0.0019	0.0022	0.0021	0.0025	0.0042
RC-P	Obj Mean	-4.238	-12.20	-13.54	-31.62	-73.31	-142.7
	Obj Median	-4.307	-12.20	-13.57	-31.71	-73.38	-142.7
	% Feasible	100%	100%	100%	100%	100%	100%
	Time (Sec)	0.0045	0.0055	0.0050	0.0050	0.0065	0.0090
	Time (Sec)	0.0045	0.0055	0.0050	0.0050	0.0065	0.0090
LT	Obj Mean	-4.302	-12.98	-13.65	-31.34	-72.36	-142.6
	Obj Median	-4.319	-13.03	-13.77	-31.61	-72.48	-142.6
	% Feasible	98%	98%	93%	95%	94%	100%
	Time (Sec)	0.0020	0.0020	0.0023	0.0022	0.0026	0.0047
	Time (Sec)	0.0020	0.0020	0.0023	0.0022	0.0026	0.0047
LT-P	Obj Mean	-4.301	-12.98	-13.65	-31.34	-72.36	-142.6
	Obj Median	-4.316	-13.03	-13.77	-31.61	-72.48	-142.6
	% Feasible	100%	100%	100%	100%	100%	100%
	Time (Sec)	0.0056	0.0055	0.0100	0.0064	0.0063	0.0086
	Time (Sec)	0.0056	0.0055	0.0100	0.0064	0.0063	0.0086
EX	Obj Mean	-5.120	-15.93	-20.79	—	—	—
	Obj Median	-5.130	-15.96	-20.78	—	—	—
	% Feasible	100%	100%	100%	—	—	—
	Time (Sec)	8.728	1520	1237	—	—	—
	Time (Sec)	8.728	1520	1237	—	—	—
RR	Obj Mean	-5.179	-16.17	-21.92	-46.73	-106.5	-213.3
	Obj Median	-5.217	-16.21	-21.89	-46.76	-106.5	-213.3
	% Feasible	0%	0%	0%	0%	0%	0%
	Time (Sec)	0.417	0.440	0.583	0.846	2.639	8.874
	Time (Sec)	0.417	0.440	0.583	0.846	2.639	8.874
N1	Obj Mean	9.8e7	1.7e17	1.5e18	—	—	—
	Obj Median	9.600	2.4e17	1.4e18	—	—	—
	% Feasible	100%	100%	100%	—	—	—
	Time (Sec)	0.415	0.498	104.2	—	—	—
	Time (Sec)	0.415	0.498	104.2	—	—	—

It is worth noting that some of the objective values are extremely large. This occurs when the baseline methods, such as EX and N1, generate poor-quality feasible solutions, particularly for larger problem instances. Due to the absence of explicit bounds on the decision variables, the baselines occasionally produce trivial yet suboptimal solutions, leading to inflated objective values. This issue is not confined to this particular case but also appears in other problem instances, further underscoring the limitations of the baseline methods in handling larger-scale optimization tasks effectively.

Q1. How do learning-based methods compare to traditional solvers and heuristics? Traditional methods (EX, RR, and N1) struggle on larger instances, often failing to return solutions within the 1000-second limit, whereas RC and LT remain effective. While N1 can find feasible solutions quickly for small instances, it suffers from numerical instability and breaks down on larger scales larger problems. Similarly, RR, which relies on relaxation rounding, struggles with feasibility across all problem scales. In contrast, RC and LT achieve objective values close to the exact

Table 3: Results for the INPs. See the caption of Table 2 for details. “% Solved” denotes the percentage of instances where a solution—whether feasible or infeasible—was found within the time limit.

Method	Metric	20×20	50×50	100×100	200×200	500×500	1000×1000
RC	Obj Mean	0.228	0.771	1.664	1.472	0.526	1.422
	Obj Median	0.217	0.752	1.594	1.436	0.526	0.809
	% Feasible	100%	98%	100%	99%	96%	97%
	Time (Sec)	0.0019	0.0020	0.0022	0.0022	0.0029	0.0040
	Time (Sec)	0.0019	0.0020	0.0022	0.0022	0.0029	0.0040
RC-P	Obj Mean	0.228	0.772	1.664	1.471	0.524	1.423
	Obj Median	0.217	0.752	1.594	1.436	0.526	0.809
	% Feasible	100%	100%	100%	100%	100%	100%
	Time (Sec)	0.0045	0.0058	0.0060	0.0054	0.0061	0.0115
	Time (Sec)	0.0045	0.0058	0.0060	0.0054	0.0061	0.0115
LT	Obj Mean	0.195	0.580	0.669	-0.356	-1.374	-3.744
	Obj Median	0.175	0.566	0.649	-0.373	-1.594	-3.716
	% Feasible	99%	98%	96%	100%	98%	99%
	Time (Sec)	0.0019	0.0020	0.0021	0.0023	0.0029	0.0050
	Time (Sec)	0.0019	0.0020	0.0021	0.0023	0.0029	0.0050
LT-P	Obj Mean	0.195	0.580	0.669	-0.356	-1.374	-3.744
	Obj Median	0.175	0.566	0.649	-0.373	-1.594	-3.716
	% Feasible	100%	100%	100%	100%	100%	100%
	Time (Sec)	0.0048	0.0050	0.0058	0.0056	0.0072	0.0117
	Time (Sec)	0.0048	0.0050	0.0058	0.0056	0.0072	0.0117
EX	Obj Mean	-0.453	1.649	256.93	—	—	—
	Obj Median	-0.463	-0.052	134.62	—	—	—
	% Feasible	100%	100%	14%	—	—	—
	% Solved	100%	100%	14%	0%	0%	0%
	Time (Sec)	0.9949	1001	1001	—	—	—
RR	Obj Mean	-0.464	-1.039	-2.068	-3.990	-9.391	—
	Obj Median	-0.476	-1.215	-2.307	-4.327	-9.221	—
	% Feasible	3%	0%	0%	0%	0%	—
	% Solved	100%	100%	100%	100%	100%	0%
	Time (Sec)	0.996	1.189	4.600	54.01	449.0	—
N1	Obj Mean	2.1e4	3.7e6	4411	—	—	—
	Obj Median	2.222	45.85	155.2	—	—	—
	% Feasible	100%	100%	14%	—	—	—
	% Solved	100%	100%	14%	0%	0%	0%
	Time (Sec)	0.144	8.968	940.4	—	—	—

Table 4: Results for the MIRBs. See the caption of Table 3 for details.

Method	Metric	2×4	20×4	200×4	2000×4	20000×4
RC	Obj Mean	23.27	59.39	503.5	5938	6.7e4
	Obj Median	21.48	48.86	461.7	5792	6.7e4
	% Feasible	97%	100%	99%	99%	76%
	Time (Sec)	0.0019	0.0019	0.0021	0.0033	0.0121
	Time (Sec)	0.0019	0.0019	0.0021	0.0033	0.0121
RC-P	Obj Mean	23.50	59.39	504.2	5942	9.8e4
	Obj Median	21.48	48.86	461.7	5792	7.3e4
	% Feasible	100%	100%	100%	100%	100%
	Time (Sec)	0.0062	0.0048	0.0052	0.0070	0.0824
	Time (Sec)	0.0062	0.0048	0.0052	0.0070	0.0824
LT	Obj Mean	23.18	62.51	622.8	5612	4.8e4
	Obj Median	20.80	63.40	626.0	5558	3.5e4
	% Feasible	98%	100%	100%	97%	66%
	Time (Sec)	0.0019	0.0020	0.0026	0.0030	0.0127
	Time (Sec)	0.0019	0.0020	0.0026	0.0030	0.0127
LT-P	Obj Mean	23.33	62.51	622.8	5615	8.0e4
	Obj Median	20.80	63.40	626.0	5558	4.5e4
	% Feasible	100%	100%	100%	100%	100%
	Time (Sec)	0.0062	0.0055	0.0062	0.0071	0.0639
	Time (Sec)	0.0062	0.0055	0.0062	0.0071	0.0639
EX	Obj Mean	19.62	64.67	8.4e5	4.7e10	1.1e15
	Obj Median	18.20	59.16	908.8	9262	1.0e5
	% Feasible	100%	100%	100%	96%	78%
	% Solved	100%	100%	100%	96%	78%
	Time (Sec)	3.5090	1005	1002	1002	1040
RR	Obj Mean	22.24	1.2e4	1.4e4	2.1e6	1.7e8
	Obj Median	22.19	51.17	501.9	5437	7.0e6
	% Feasible	55%	59%	40%	6%	18%
	% Solved	100%	100%	58%	7%	22%
	Time (Sec)	0.1805	0.5570	1.2396	9.2334	1064
N1	Obj Mean	40.37	87.83	3.7e8	8.3e12	1.2e15
	Obj Median	27.93	77.34	957.4	9379	1.0e5
	% Feasible	100%	100%	100%	95%	78%
	% Solved	100%	100%	100%	95%	78%
	Time (Sec)	0.0323	0.0813	0.2608	71.91	782.1

solver (EX) while maintaining lower infeasibility rates and achieving several orders of magnitude speed-ups. For IQPs and INPs, RC and LT outperform heuristic baselines such

as N1 and RR, especially as problem sizes increase. In MIRBs, they even surpass EX in most cases. Overall, our learning-based approaches provide substantial advantages in scalability, speed, and solution quality over exact solvers and heuristic methods.

Q2. How effective is the integer feasibility projection?

Despite the lack of theoretical convergence guarantees, learning-based methods with feasibility projection (RC-P and LT-P) successfully find feasible solutions for all test instances. As shown in Appendix E.1, constraint violations in RC and LT in IQPs and INPs are sparse and minor, which allows the projection step to correct infeasibilities with negligible impact on the objective value. For MIRBs, feasibility projection plays an even more crucial role—while feasibility rates decline significantly for RC and LT as the problem size grows to 20,000 variables, applying feasibility projection allows RC-P and LT-P to satisfy all constraints across all instances. Although feasibility projection introduces additional computational overhead, inference remains highly efficient. Even with projection, total inference time remains below one second, preserving a substantial speed advantage over other methods. Thus, these results demonstrate both the effectiveness and computational efficiency of our gradient-based projection step.

Q3. How does the choice of penalty weight affect performance?

The penalty weight (λ in Equation (2)) is a critical hyperparameter that influences the trade-off between solution feasibility and objective value. We analyze its effect using the 1000×1000 INPs, evaluating RC, LT, RC-P, and LT-P under penalty weights ranging from 0.1 to 1000. Additional results for the 1000×1000 IQPs, the 2000×4 MIRBs, and smaller-scale instances compared against exact solvers are provided in Appendix F.2. Figure 3 reveals an inherent trade-off between achieving a higher proportion of feasible solutions and maintaining lower objective values prior to the application of feasibility projection. Lower yet reasonable penalty weights may lead to solutions that violate constraints. Surprisingly, After applying the feasibility projection (RC-P and LT-P), the high infeasibility rates observed with smaller penalty weights can be resolved, while the lower objective values achieved by these weights remain largely intact. Further experiments in Appendix F.2 exhibit similar trends across different problem types and scales. This suggests that selecting lower penalty weights for RC-P and LT-P than those used in the main experiments could further improve results.

Q4. How long is the training time? In addition to evaluating solution quality, feasibility, and solving/inference times, we also measured the offline training times for our two approaches on different problem sizes. These results, along with training times for other problem types, are presented

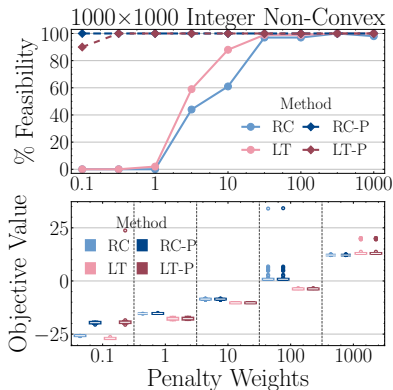


Figure 3: Illustration of the proportion of feasible solutions (Top) and objective value (Bottom) on the test set. As the penalty weight increases, the fraction of feasible solutions increases while the objective value generally deteriorates.

in Appendix E.2, where it is evident that the training times for the learning-based methods scale well with problem size. Compared to the runtime of exact solvers, the training process is relatively short, often requiring only a few minutes for smaller instances and a few hours for the largest problems. In some cases, training even takes less time than finding the first feasible solution for a single instance with the exact solver. Moreover, when repeatedly solving multiple instances, the training cost can be amortized, making our approach particularly advantageous in real-world scenarios where rapid deployment and large-scale optimization are required.

6. Conclusion

We introduced the first general learning-to-optimize method for parametric MINLPs, featuring rounding correction layers that enable neural networks to generate high-quality mixed-integer solutions while preserving gradient information for training. Our self-supervised approach does not require collecting optimal solutions as labels, substantially reducing data preparation efforts. Furthermore, we proposed a feasibility projection as post-processing to improve constraint satisfaction with negligible computational overhead.

The experiments demonstrate that our learning-based methods outperform traditional solvers and other heuristics across various problem types. Despite the complexity of these tasks, our methods maintain strong performance in terms of both feasibility and solution quality, particularly in high-dimensional settings where traditional approaches often fail to produce solutions within a reasonable time. To our knowledge, our work is the first to tackle learning for parametric MINLPs and successfully solve one of the largest MINLPs reported to date.

Although our methods demonstrate strong performance, cer-

tain limitations remain. Specifically, while no infeasible instances were observed after feasibility projection in our experiments, theoretical guarantees are still lacking. One promising direction is to establish convergence guarantees by interpreting the feasibility projection step as a special case of Projected Gradient Descent (PGD) and analyzing its behavior for specific classes. Additionally, future work could explore alternative strategies to enhance feasibility. For example, in certain problem classes, a subset of constraints could be directly handled using differentiable optimization layers (Agrawal et al., 2019) while others are incorporated into the loss function. Additionally, specialized neural network architectures, such as those proposed by Pan et al. (2020) and Tordesillas et al. (2023), could be designed to satisfy certain types of constraints inherently.

References

- Agrawal, A., Amos, B., Barratt, S., Boyd, S., Diamond, S., and Kolter, Z. Differentiable convex optimization layers. *ArXiv*, abs/1910.12430, 2019.
- Alvarez, A. M., Louveaux, Q., and Wehenkel, L. A machine learning-based approximation of strong branching. *INFORMS Journal on Computing*, 29(1):185–195, 2017.
- Amos, B. Tutorial on amortized optimization for learning to optimize over continuous domains. *CoRR*, abs/2202.00665, 2022. URL <https://arxiv.org/abs/2202.00665>.
- Amos, B. and Kolter, J. Z. Optnet: Differentiable optimization as a layer in neural networks. In *International conference on machine learning*, pp. 136–145. PMLR, 2017.
- Baltean-Lugojan, R., Bonami, P., Misener, R., and Tramtantani, A. Scoring positive semidefinite cutting planes for quadratic optimization via trained neural networks. <https://optimization-online.org/2018/11/6943/>, 2019.
- Belotti, P., Lee, J., Liberti, L., Margot, F., and Wächter, A. Branching and bounds tightening techniques for non-convex MINLP. *Optimization Methods & Software*, 24(4-5):597–634, 2009.
- Bengio, Y., Léonard, N., and Courville, A. Estimating or propagating gradients through stochastic neurons for conditional computation. *arXiv preprint arXiv:1308.3432*, 2013.
- Bengio, Y., Lodi, A., and Prouvost, A. Machine learning for combinatorial optimization: a methodological tour d’horizon. *European Journal of Operational Research*, 290(2):405–421, 2021.
- Berthet, Q., Blondel, M., Teboul, O., Cuturi, M., Vert, J.-P., and Bach, F. Learning with differentiable perturbed optimizers. *Advances in neural information processing systems*, 33:9508–9519, 2020.
- Berthold, T. Rens: the optimal rounding. *Mathematical Programming Computation*, 6:33–54, 2014.
- Berthold, T. and Hendel, G. Learning to scale mixed-integer programs. In *Proceedings of the AAAI Conference on Artificial Intelligence*, 2021.
- Bertsimas, D. and Stellato, B. Online mixed-integer optimization in milliseconds. *INFORMS Journal on Computing*, 34(4):2229–2248, 2022.
- Bestuzheva, K., Besançon, M., Chen, W.-K., Chmiela, A., Donkiewicz, T., van Doornmalen, J., Eifler, L., Gaul, O., Gamrath, G., Gleixner, A., et al. The scip optimization suite 8.0. *arXiv preprint arXiv:2112.08872*, 2021.
- Bolusani, S., Besançon, M., Gleixner, A., Berthold, T., D’Ambrosio, C., Muñoz, G., Paat, J., and Thomopoulos, D. The MIP Workshop 2023 computational competition on reoptimization, 2023. URL <http://arxiv.org/abs/2311.14834>.
- Bonami, P., Lodi, A., and Zarpellon, G. A classifier to decide on the linearization of mixed-integer quadratic problems in cplex. *Operations research*, 70(6):3303–3320, 2022.
- Cauligi, A., Culbertson, P., Schmerling, E., Schwager, M., Stellato, B., and Pavone, M. Coco: Online mixed-integer control via supervised learning. *IEEE Robotics and Automation Letters*, 7(2):1447–1454, 2021.
- Chen, T., Chen, X., Chen, W., Heaton, H., Liu, J., Wang, Z., and Yin, W. Learning to optimize: A primer and a benchmark. *Journal of Machine Learning Research*, 23(189):1–59, 2022.
- Chen, W., Tanneau, M., and Van Hentenryck, P. End-to-end feasible optimization proxies for large-scale economic dispatch. *IEEE Transactions on Power Systems*, 39(2):4723–4734, 2024. doi: 10.1109/TPWRS.2023.3317352.
- Chmiela, A., Khalil, E., Gleixner, A., Lodi, A., and Pokutta, S. Learning to schedule heuristics in branch and bound. *Advances in Neural Information Processing Systems*, 34:24235–24246, 2021.
- Crama, Y., Kolen, A. W., and Pesch, E. Local search in combinatorial optimization. *Artificial Neural Networks: An Introduction to ANN Theory and Practice*, pp. 157–174, 2005.

- Dai, H., Khalil, E., Zhang, Y., Dilkina, B., and Song, L. Learning combinatorial optimization algorithms over graphs. *Advances in neural information processing systems*, 30, 2017.
- Deza, A. and Khalil, E. B. Machine learning for cutting planes in integer programming: A survey. In *Proceedings of the Thirty-Second International Joint Conference on Artificial Intelligence, IJCAI-2023*. International Joint Conferences on Artificial Intelligence Organization, August 2023. doi: 10.24963/ijcai.2023/739. URL <http://dx.doi.org/10.24963/IJCAI.2023/739>.
- Ding, J.-Y., Zhang, C., Shen, L., Li, S., Wang, B., Xu, Y., and Song, L. Accelerating primal solution findings for mixed integer programs based on solution prediction. In *Proceedings of the AAAI Conference on Artificial Intelligence*, 2020.
- Djolonga, J. and Krause, A. Differentiable learning of submodular models. *Advances in Neural Information Processing Systems*, 30, 2017.
- Donti, P., Amos, B., and Kolter, J. Z. Task-based end-to-end model learning in stochastic optimization. *Advances in neural information processing systems*, 30, 2017.
- Donti, P., Rolnick, D., and Kolter, J. Z. DC3: A learning method for optimization with hard constraints. In *International Conference on Learning Representations*, 2021.
- Dragotto, G., Clarke, S., Fisac, J. F., and Stellato, B. Differentiable cutting-plane layers for mixed-integer linear optimization, 2023. URL <https://arxiv.org/abs/2311.03350>.
- Drgona, J., Tuor, A., Koch, J., Shapiro, M., Jacob, B., and Vrabie, D. Neuromancer: Neural modules with adaptive nonlinear constraints and efficient regularizations, 2023. URL <https://github.com/pnml/neuromancer>.
- Ferber, A. M., Huang, T., Zha, D., Schubert, M., Steiner, B., Dilkina, B., and Tian, Y. Surco: Learning linear surrogates for combinatorial nonlinear optimization problems. In *International Conference on Machine Learning*, pp. 10034–10052. PMLR, 2023.
- Fioretto, F., Mak, T. W., and Van Hentenryck, P. Predicting ac optimal power flows: Combining deep learning and lagrangian dual methods. In *Proceedings of the AAAI conference on artificial intelligence*, 2020.
- Fischetti, M., Glover, F., and Lodi, A. The feasibility pump. *Mathematical Programming*, 104:91–104, 2005.
- Fletcher, R. and Leyffer, S. Solving mixed integer nonlinear programs by outer approximation. *Mathematical programming*, 66:327–349, 1994.
- Gasse, M., Chételat, D., Ferroni, N., Charlin, L., and Lodi, A. Exact combinatorial optimization with graph convolutional neural networks. *Advances in neural information processing systems*, 32, 2019.
- Gleixner, A., Hendel, G., Gamrath, G., Achterberg, T., Bastubbe, M., Berthold, T., Christophel, P., Jarck, K., Koch, T., Linderoth, J., et al. Miplib 2017: data-driven compilation of the 6th mixed-integer programming library. *Mathematical Programming Computation*, 13(3): 443–490, 2021.
- Gurobi Optimization, LLC. Gurobi Optimizer Reference Manual, 2021. URL <https://www.gurobi.com>.
- He, H., Daume III, H., and Eisner, J. M. Learning to search in branch and bound algorithms. *Advances in neural information processing systems*, 27, 2014.
- Hendriks, J., Jidling, C., Wills, A., and Schön, T. Linearly constrained neural networks. *arXiv preprint arXiv:2002.01600*, 2020.
- Hentenryck, P. V. Optimization learning, 2025. URL <https://arxiv.org/abs/2501.03443>.
- Hopfield, J. J. and Tank, D. W. “neural” computation of decisions in optimization problems. *Biological cybernetics*, 52(3):141–152, 1985.
- Huang, T., Ferber, A. M., Tian, Y., Dilkina, B., and Steiner, B. Searching large neighborhoods for integer linear programs with contrastive learning. In *International Conference on Machine Learning*, pp. 13869–13890. PMLR, 2023.
- Jang, E., Gu, S., and Poole, B. Categorical reparameterization with gumbel-softmax. *arXiv preprint arXiv:1611.01144*, 2016.
- Jia, Z., Huang, X., Eric, I., Chang, C., and Xu, Y. Constrained deep weak supervision for histopathology image segmentation. *IEEE transactions on medical imaging*, 36(11):2376–2388, 2017.
- Johnson, D. S. and McGeoch, L. A. The traveling salesman problem: a case study. *Local search in combinatorial optimization*, pp. 215–310, 1997.
- Kervadec, H., Dolz, J., Yuan, J., Desrosiers, C., Granger, E., and Ayed, I. B. Constrained deep networks: Lagrangian optimization via log-barrier extensions. In *2022 30th European Signal Processing Conference (EUSIPCO)*, pp. 962–966. IEEE, 2022.

- Khalil, E., Le Bodic, P., Song, L., Nemhauser, G., and Dilkina, B. Learning to branch in mixed integer programming. In *Proceedings of the AAAI Conference on Artificial Intelligence*, 2016.
- Khalil, E., Morris, C., and Lodi, A. MIP-GNN: A data-driven framework for guiding combinatorial solvers. In *Proceedings of the AAAI Conference on Artificial Intelligence*, 2022.
- King, E., Kotary, J., Fioretto, F., and Drgona, J. Metric learning to accelerate convergence of operator splitting methods for differentiable parametric programming, 2024. URL <https://arxiv.org/abs/2404.00882>.
- Kleinert, T., Labbé, M., Ljubić, I., and Schmidt, M. A survey on mixed-integer programming techniques in bilevel optimization. *EURO Journal on Computational Optimization*, 9:100007, 2021.
- Kotary, J., Fioretto, F., and Van Hentenryck, P. Learning hard optimization problems: A data generation perspective. *Advances in Neural Information Processing Systems*, 34:24981–24992, 2021a.
- Kotary, J., Fioretto, F., Van Hentenryck, P., and Wilder, B. End-to-end constrained optimization learning: A survey. *arXiv preprint arXiv:2103.16378*, 2021b.
- Land, A. H. and Doig, A. G. *An automatic method for solving discrete programming problems*. Springer, 2010.
- Li, M., Kolouri, S., and Mohammadi, J. Learning to solve optimization problems with hard linear constraints. *IEEE Access*, 11:59995–60004, 2022. URL <https://api.semanticscholar.org/CorpusID:251741205>.
- Lundell, A. and Kronqvist, J. Polyhedral approximation strategies for nonconvex mixed-integer nonlinear programming in shot. *Journal of Global Optimization*, 82(4):863–896, 2022.
- Marcucci, T. and Tedrake, R. Warm start of mixed-integer programs for model predictive control of hybrid systems. *IEEE Transactions on Automatic Control*, 66(6):2433–2448, 2020.
- Márquez-Neila, P., Salzmann, M., and Fua, P. Imposing hard constraints on deep networks: Promises and limitations. *arXiv preprint arXiv:1706.02025*, 2017.
- Nair, V., Bartunov, S., Gimeno, F., von Glehn, I., Lichocki, P., Lobov, I., O’Donoghue, B., Sonnerat, N., Tjandraatmadja, C., Wang, P., et al. Solving mixed integer programs using neural networks. *arXiv preprint arXiv:2012.13349*, 2020.
- Nazir, N. and Almassalkhi, M. Guaranteeing a physically realizable battery dispatch without charge-discharge complementarity constraints. *IEEE Transactions on Smart Grid*, 14(3):2473–2476, 2021.
- Nowak, A., Villar, S., Bandeira, A. S., and Bruna, J. Revised note on learning quadratic assignment with graph neural networks. In *2018 IEEE Data Science Workshop (DSW)*, pp. 1–5. IEEE, 2018.
- Nowak, I. *Relaxation and decomposition methods for mixed integer nonlinear programming*, volume 152. Springer Science & Business Media, 2005.
- Pan, X., Zhao, T., Chen, M., and Zhang, S. Deepopf: A deep neural network approach for security-constrained dc optimal power flow. *IEEE Transactions on Power Systems*, 36(3):1725–1735, 2020.
- Paszke, A., Gross, S., Massa, F., Lerer, A., Bradbury, J., Chanan, G., Killeen, T., Lin, Z., Gimelshein, N., Antiga, L., et al. Pytorch: An imperative style, high-performance deep learning library. In *Advances in Neural Information Processing Systems*, pp. 8024–8035, 2019.
- Pathak, D., Krahenbuhl, P., and Darrell, T. Constrained convolutional neural networks for weakly supervised segmentation. In *Proceedings of the IEEE international conference on computer vision*, pp. 1796–1804, 2015.
- Pogančić, M. V., Paulus, A., Musil, V., Martius, G., and Rolinek, M. Differentiation of blackbox combinatorial solvers. In *International Conference on Learning Representations*, 2020.
- Sambharya, R., Hall, G., Amos, B., and Stellato, B. End-to-end learning to warm-start for real-time quadratic optimization. In *Learning for Dynamics and Control Conference*, pp. 220–234. PMLR, 2023.
- Schouwenaars, T., De Moor, B., Feron, E., and How, J. Mixed integer programming for multi-vehicle path planning. In *2001 European control conference (ECC)*, pp. 2603–2608. IEEE, 2001.
- Song, J., Yue, Y., Dilkina, B., et al. A general large neighborhood search framework for solving integer linear programs. *Advances in Neural Information Processing Systems*, 33:20012–20023, 2020.
- Sonnerat, N., Wang, P., Ktena, I., Bartunov, S., and Nair, V. Learning a large neighborhood search algorithm for mixed integer programs. *arXiv preprint arXiv:2107.10201*, 2021.
- Tang, B. and Khalil, E. B. Cave: A cone-aligned approach for fast predict-then-optimize with binary linear programs.

- In *International Conference on the Integration of Constraint Programming, Artificial Intelligence, and Operations Research*, pp. 193–210. Springer, 2024.
- Tordesillas, J., How, J. P., and Hutter, M. Rayen: Imposition of hard convex constraints on neural networks. *arXiv preprint arXiv:2307.08336*, 2023.
- Vinyals, O., Fortunato, M., and Jaitly, N. Pointer networks. *Advances in neural information processing systems*, 28, 2015.
- Wächter, A. and Biegler, L. T. On the implementation of an interior-point filter line-search algorithm for large-scale nonlinear programming. *Mathematical programming*, 106:25–57, 2006.
- Wilder, B., Dilkina, B., and Tambe, M. Melding the data-decisions pipeline: Decision-focused learning for combinatorial optimization. In *Proceedings of the AAAI Conference on Artificial Intelligence*, 2019.
- Xu, L., Hutter, F., Hoos, H. H., and Leyton-Brown, K. Hydra-mip: Automated algorithm configuration and selection for mixed integer programming. In *RCRA workshop on experimental evaluation of algorithms for solving problems with combinatorial explosion at the international joint conference on artificial intelligence (IJCAI)*, pp. 16–30, 2011.
- Ye, H., Xu, H., and Wang, H. Light-milpopt: Solving large-scale mixed integer linear programs with lightweight optimizer and small-scale training dataset. In *The Twelfth International Conference on Learning Representations*, 2024.
- Zarpellon, G., Jo, J., Lodi, A., and Bengio, Y. Parameterizing branch-and-bound search trees to learn branching policies. In *Proceedings of the AAAI Conference on Artificial Intelligence*, 2021.
- Zhang, J., Liu, C., Li, X., Zhen, H.-L., Yuan, M., Li, Y., and Yan, J. A survey for solving mixed integer programming via machine learning. *Neurocomputing*, 519:205–217, 2023.

A. Details of Correction Layers

The following subsections detail the two distinct approaches for designing the correction layer φ_{Θ_2} while sharing the same network π_{Θ_1} for generating relaxed solutions $\bar{\mathbf{x}}^i$ in both methods. The workflow for each approach is illustrated in Figure 4.

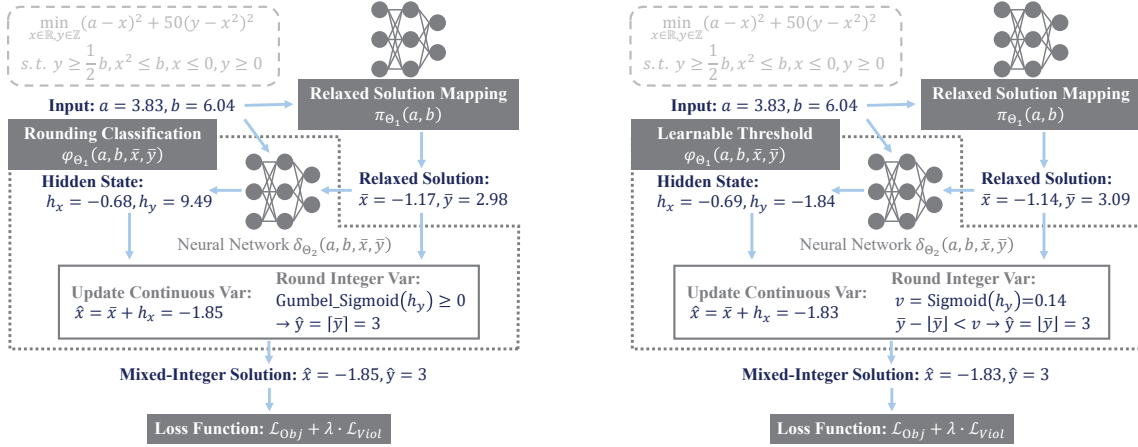


Figure 4: Examples of the two integer correction layers: Rounding Classification (left) uses a classification-based rounding strategy, while Learnable Threshold (right) yields a threshold to guide rounding decisions.

Rounding Classification. The key step of the *Rounding Classification* (RC) approach is performed in line 6 of Algorithm 1. For the integer variables, RC applies a stochastic soft-rounding mechanism to the neural network output $\mathbf{h}_z^i = \delta_{\Theta_2}(\bar{\mathbf{x}}^i, \boldsymbol{\xi}^i)$, producing a binary vector $\mathbf{b}^i \in \{0, 1\}^{n_z}$. Each entry of \mathbf{b}^i determines whether the fractional part of the relaxed value $\bar{\mathbf{x}}_z^i$ is rounded down (0) or up (1).

To introduce stochasticity and enhance exploration during training, the Gumbel-noise method (Jang et al., 2016) is employed. Specifically, logits \mathbf{h}_z^i are perturbed by noise sampled from the Gumbel distribution:

$$\epsilon = -\log(-\log(U)), \quad U \sim \text{Uniform}(0, 1).$$

where U is a random variable drawn from the uniform distribution over the interval $[0, 1]$. The perturbed logits are then passed through the Sigmoid function to compute the probabilities for rounding:

$$\text{Gumbel-Sigmoid}(h) = \frac{1}{1 + \exp\left(-\frac{h + \epsilon_1 - \epsilon_2}{\tau}\right)}$$

where ϵ_1 and ϵ_2 are independent Gumbel samples, and $\tau > 0$ is the temperature parameter controlling the smoothness of the approximation. A smaller τ produces sharper transitions, approaching a hard step function, while larger τ yields smoother probabilistic behavior. Finally, a hard binarization step is applied using the STE to ensure discrete binary outputs in the forward pass while retaining gradients for backpropagation.

Finally, a hard binarization step is applied using the STE, ensuring discrete binary outputs in the forward pass while retaining gradients during backpropagation. This combination allows the RC method to refine integer decisions while facilitating gradient-based optimization. In our experiments, we set $\tau = 1$ for simplicity.

Learnable Threshold. The *Learnable Threshold* (LT) approach, detailed in lines 8 and 9 of Algorithm 1, provides an alternative correction strategy. Instead of relying on probability as in RC, LT learns to predict a vector of per-variable thresholds $\mathbf{v}^i \in [0, 1]^{n_z}$, which are used to guide the rounding process. A variable is rounded up if the fractional part of its relaxed value $(\bar{\mathbf{x}}_z^i - \hat{\mathbf{x}}_z^i)$ exceeds the threshold \mathbf{v}^i . The rounding decision is computed via the indicator function:

$$\mathbf{b}^i \leftarrow \mathbb{I}((\bar{\mathbf{x}}_z^i - \hat{\mathbf{x}}_z^i) - \mathbf{v}^i > 0)$$

which produces binary outputs in the forward pass. To ensure differentiability, the gradient is approximated by the Sigmoid function:

$$\mathbf{b}_{\text{Soft}}^i \leftarrow \frac{1}{1 + \exp\left(-10 \cdot (\bar{\mathbf{x}}_z^i - \hat{\mathbf{x}}_z^i - \mathbf{v}^i)\right)}$$

Here, the slope is set to 10 to sharpen the Sigmoid function.

B. Example Illustration

This section illustrates the process of our Integer Correction and Feasibility Projection components in producing solutions. We present a two-dimensional Mixed-Integer Rosenbrock Benchmark (MIRB) instance, formulated as follows:

$$\begin{aligned} \min_{x \in \mathbb{R}, y \in \mathbb{Z}} \quad & (a - x)^2 + 50(y - x^2)^2 \\ \text{subject to} \quad & y \geq b/2, \quad x^2 \leq b, \quad x \leq 0, \quad y \geq 0. \end{aligned}$$

In this formulation, x is a continuous decision variable, while y is an integer decision variable. Both variables are subject to linear constraints. The instance parameters a and b serve as input features to the neural network.

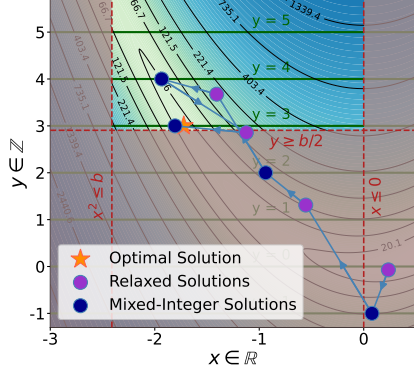


Figure 5: Example of the relaxed solutions \bar{x}, \bar{y} and the mixed-integer solutions \hat{x}, \hat{y} across different epochs of training for the same sample instance using RC.

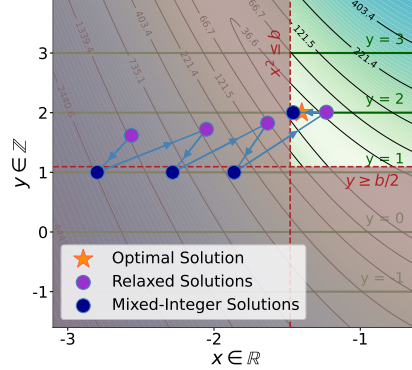


Figure 6: Example of the relaxed solutions \bar{x}, \bar{y} and the mixed-integer solutions \hat{x}, \hat{y} across different iterations of feasibility projection to refine an infeasible solution.

Integer Correction Layer Figure 5 illustrates the progression of relaxed solutions (\bar{x}, \bar{y}) and their corresponding mixed-integer solutions (\hat{x}, \hat{y}) across different training epochs. In this example, the instance parameters are set to $a = 3.83$ and $b = 6.04$. Throughout training, the relaxed solutions (\bar{x}, \bar{y}) are iteratively adjusted by the neural network, and the integer correction layer transforms them into mixed-integer solutions. As training progresses, the model learns to generate solutions that are not only integer-feasible but also of high quality in terms of the objective function and constraint satisfaction.

Integer Feasible Projection Figure 6 illustrates the iterative refinement process of the feasibility projection step, applied to an initially infeasible solution. In this example, the instance parameters are set to $a = 4.16$ and $b = 2.19$. The relaxed solution (\bar{x}, \bar{y}) is iteratively adjusted through gradient-based updates, reducing constraint violations while preserving the integer feasibility enforced by the correction layer. As the projection process progresses, the solution moves towards the feasible region, forcing that the final mixed-integer solution (\hat{x}, \hat{y}) satisfies all constraints.

C. MINLP Problem Setup and Parameter Sampling

C.1. Integer Quadratic Problems

The integer quadratic problems (IQPs) used in our experiments are formulated as follows:

$$\min_{\mathbf{x} \in \mathbb{Z}^n} \quad \frac{1}{2} \mathbf{x}^T \mathbf{Q} \mathbf{x} + \mathbf{p}^T \mathbf{x} \quad \text{subject to} \quad \mathbf{A} \mathbf{x} \leq \mathbf{b}$$

where the coefficients $\mathbf{Q} \in \mathbb{R}^{n \times n}$, $\mathbf{p} \in \mathbb{R}^n$, and $\mathbf{A} \in \mathbb{R}^{m \times n}$ were fixed, while $\mathbf{b} \in \mathbb{R}^m$ were treated as a parametric input, varying between instances to represent different optimization scenarios.

To ensure convexity, $\mathbf{Q} \in \mathbb{R}^{n \times n}$ is a diagonal matrix with entries sampled uniformly from $[0, 0.01]$. The linear coefficient vector $\mathbf{p} \in \mathbb{R}^n$ has entries drawn from a uniform distribution over $[0, 0.1]$, while the constraint matrix $\mathbf{A} \in \mathbb{R}^{m \times n}$ is generated from a normal distribution with a mean of 0 and a standard deviation of 0.1. The parameter $\mathbf{b} \in \mathbb{R}^m$, representing

the right-hand side of the inequality constraints, is sampled uniformly from $[-1, 1]$. These variations in \mathbf{b} across instances ensure the parametric nature of the problem.

Compared to the original setup in [Donti et al. \(2021\)](#), which focused on continuous optimization, we introduced integer constraints on all decision variables. Additionally, equality constraints were removed to ensure that generated instances remain feasible, as such constraints could lead to infeasibilities in the discrete space. These modifications preserve the fundamental structure of the original problems while ensuring compatibility with our proposed framework.

C.2. Integer Non-convex Problems

The integer non-convex problem (INPs) used in the experiments is derived by modifying the IQPs from [Appendix C.1](#) as follows:

$$\min_{\mathbf{x} \in \mathbb{Z}^n} \frac{1}{2} \mathbf{x}^\top \mathbf{Q} \mathbf{x} + \mathbf{p}^\top \sin(\mathbf{x}) \quad \text{subject to } \mathbf{A} \mathbf{x} \leq \mathbf{b}$$

where the sine function is applied element-wise to the decision variables \mathbf{x} . This introduces non-convexity into the problem, making it more challenging compared to the convex case. For the integer non-convex problems, the coefficients \mathbf{Q} , \mathbf{p} , \mathbf{A} , and \mathbf{b} are generated in the same way as in the quadratic formulation. However, an additional parameter $\mathbf{d} \in \mathbb{R}^m$ is introduced, with each element independently sampled from a uniform distribution over $[-0.5, 0.5]$. The parameter \mathbf{d} modifies the constraint matrix \mathbf{A} by adding \mathbf{d} to its first column and subtracting \mathbf{d} from its second column. Alongside \mathbf{d} , the right-hand side vector \mathbf{b} remains a dynamic parameter in the problem. The problem scale and experimental setup remain consistent with IQPs.

C.3. Mixed-integer Ronsenbrock Problems

The mixed-integer Rosenbrock problem (MIRBs) used in this study is defined as:

$$\begin{aligned} \min_{\mathbf{x} \in \mathbb{R}^n, \mathbf{y} \in \mathbb{Z}^n} & \|\mathbf{a} - \mathbf{x}\|_2^2 + 50 \|\mathbf{y} - \mathbf{x}^2\|_2^2 \\ \text{subject to } & \|\mathbf{x}\|_2^2 \leq nb, \mathbf{1}^\top \mathbf{y} \geq \frac{nb}{2}, \mathbf{p}^\top \mathbf{x} \leq 0, \mathbf{Q}^\top \mathbf{y} \leq 0, \end{aligned}$$

where $\mathbf{x} \in \mathbb{R}^n$ are continuous decision variables and $\mathbf{y} \in \mathbb{Z}^n$ are integer decision variables. The vectors $\mathbf{p} \in \mathbb{R}^n$ and $\mathbf{Q} \in \mathbb{R}^n$ are fixed for each instance, while the parameters b and \mathbf{a} vary. In detail, the vectors $\mathbf{p} \in \mathbb{R}^n$ and $\mathbf{Q} \in \mathbb{R}^n$ are generated from a standard normal distribution. The parameter b is uniformly distributed over $[1, 8]$ for each instance, and the parameter $\mathbf{a} \in \mathbb{R}^n$ represents a vector where elements drawn independently from a uniform distribution over $[0.5, 4.5]$. The parameters b and \mathbf{a} influence the shape of the feasible region and the landscape of the objective function, serving as input features to the neural network.

D. Neural Network Structure and Hyperparameters

The solution mapping π_{Θ_1} used across all learning-based methods—RC, LT, and ablation studies—consists of five fully connected layers with ReLU activations. The rounding correction network φ_{Θ_2} for RC and LT is composed of four fully connected layers, also with ReLU activations, and incorporates Batch Normalization and Dropout with a rate of 0.2 to prevent overfitting. For feasibility projection, we set a maximum iteration limit of 1000 for computational efficiency.

To accommodate varying problem complexities, hidden layer widths were scaled proportionally to the problem size:

- For the IQPs and INPs, the hidden layer width used in the learning-based methods was scaled accordingly, increasing from 64, 128 up to 2048 for the corresponding problem sizes. Smaller problems, such as 20×20 , used smaller hidden layers 64, while larger problems, such as 1000×1000 , used hidden layers with widths up to 2048 to accommodate the complexity.
- For the MIRBs, the hidden layer width was scaled based on the number of variables: a width of 4 was used for problems with 2 variables, 16 for problems with 20 variables, and up to 1024 for problems with 10,000 variables.

All networks were trained using the AdamW optimizer with learning rate 10^{-3} , batch size 64 and 200 epochs, with early stopping based on validation performance. The constraint penalty weight λ was set to 100 for all benchmark problems.

E. Additional Experimental Analyses

E.1. Constraints Violations

This section examines constraint violations across three benchmark problems, focusing on both their frequency and magnitude. To aid understanding, the results are presented using heatmaps, where each heatmap (Figure 7, Figure 8, and Figure 9) displays rows as 100 test instances and columns as individual constraints, reflecting the solutions before the application of the projection step.

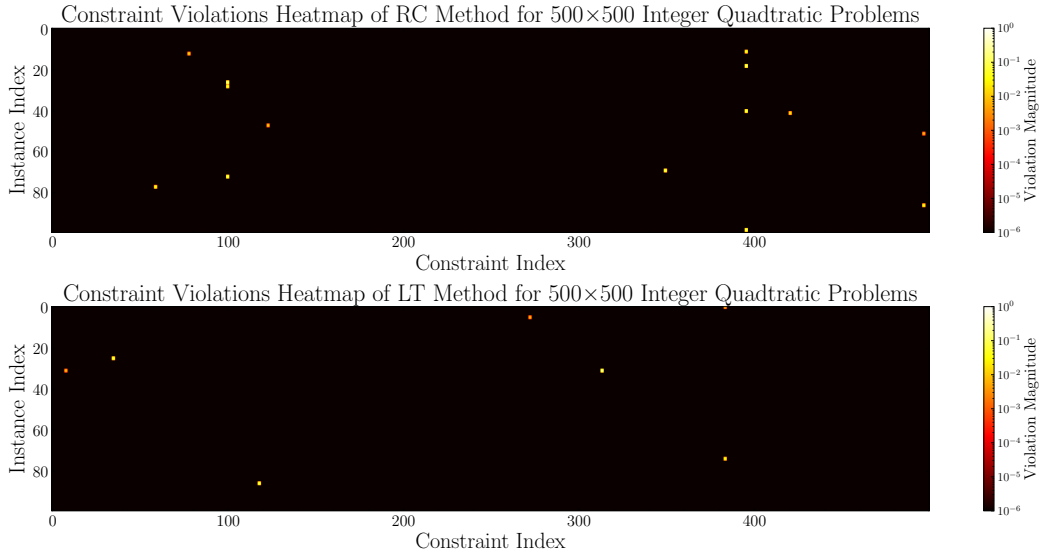


Figure 7: Illustration of Constraint Violation Heatmap of RC method (Top) and LT method (bottom) for 500×500 mixed-integer QP on 100 test instances: Each row represents an instance in the test set, while each column corresponds to a specific constraint. Color intensity indicates the magnitude of constraint violation, with lighter shades representing larger violations.

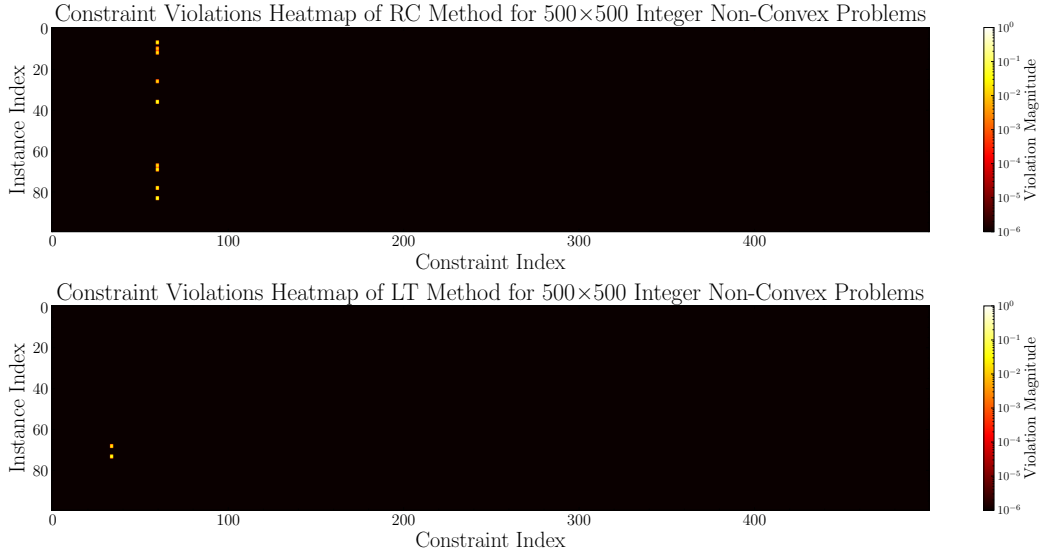


Figure 8: Illustration of Constraint Violation Heatmap of RC method (Top) and LT method (bottom) for 500×500 INPs on 100 test instances: Each row represents an instance in the test set, while each column corresponds to a specific constraint. Color intensity indicates the magnitude of constraint violation, with lighter shades representing larger violations.

The heatmaps for the IQPs (Figure 7) and the INPs (Figure 8) reveal a sparse distribution of constraint violations, primarily

concentrated in a few constraints across instances. This indicates that the majority of constraints are consistently satisfied, with violations being limited to isolated instances. Overall, the magnitude and frequency of these violations are nearly negligible. Thus, our feasibility projection effectively corrects them. In contrast, an unexpected observation is that when these near-feasible solutions are provided as warm-starting points to Gurobi or SCIP, the solvers consistently fail to recover a feasible solution, despite the minimal constraint violations.

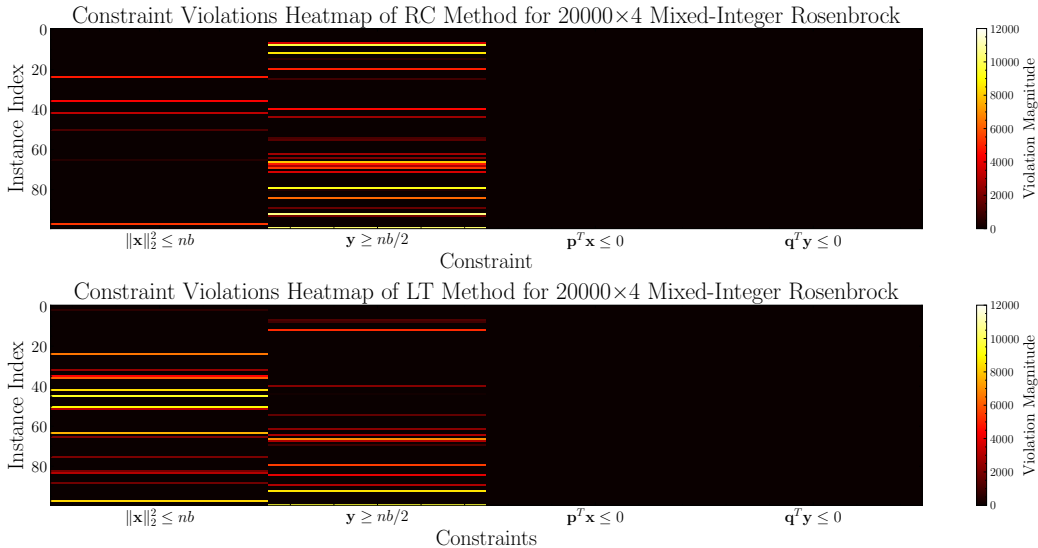


Figure 9: Illustration of Constraint Violation Heatmap of RC method (Top) and LT method (bottom) for 20000×4 MIRBs on 100 test instances: Each row represents an instance in the test set, while each column corresponds to a specific constraint. Color intensity indicates the magnitude of constraint violation, with lighter shades representing larger violations.

Figure 9 reveals a significantly denser distribution of constraint violations in the high-dimensional MIRBs, highlighting the increased complexity of this large-scale MINLP. Given the scale and difficulty of this problem, even state-of-the-art solvers fail to produce feasible solutions, and both RC and LT exhibit a high proportion of constraint violations, with magnitudes reaching the order of 10^3 . Remarkably, despite these substantial violations, Table 4 shows that the feasibility projection in RC-P and LT-P successfully restores feasibility across all 100 test instances, albeit at the cost of increased objective values.

E.2. Training Time

This section presents the training times for the RC and LT methods across various problem sizes. All training runs were conducted using datasets of 9,000 instances for each problem, with 1,000 instances reserved for validation per epoch. While the training process was set for 200 epochs, an early stopping strategy was applied, allowing the training to terminate earlier when performance plateaued. Note that RC-P and LT-P are not included in the training time comparison, as feasibility projection is applied only as a post-processing step and does not impact the training duration.

Table 5: Training Times (in seconds) for RC and LT methods across different problem sizes for the IQPs Each method was set to train for 200 epochs, with early stopping applied.

Method	20×20	50×50	100×100	200×200	500×500	1000×1000
RC	153.98	237.11	141.15	149.43	606.23	727.32
LT	154.33	158.61	128.86	139.17	458.62	462.41

Table 6: Training Times (in seconds) for RC and LT methods across different problem sizes for the INPs. Each method was set to train for 200 epochs, with early stopping applied.

Method	20×20	50×50	100×100	200×200	500×500	1000×1000
RC	173.02	138.53	136.01	104.05	116.01	156.85
LT	104.35	88.41	111.38	89.24	230.52	195.67

Table 7: Training Times (in seconds) for RC and LT methods across different problem sizes for the MIRBs. Each method was set to train for 200 epochs, with early stopping applied.

Method	2×4	20×4	200×4	2000×4	20000×4
RC	230.68	112.35	75.49	106.76	5227.05
LT	126.60	125.11	86.43	84.61	6508.41

Table 5, Table 6, and Table 7 summarize the training times (in seconds) required by each method for problems of different scales. These results highlight the computational efficiency of our methods during training, with training times for most problem instances remaining within a few hundred seconds. Even for large-scale problems, such as the 20000×4 MIRBs, RC and LT required only a few hours of training—much shorter than the time exact solvers take to find just a single feasible solution for an instance.

F. Additional Experiments

F.1. Ablation Study

To evaluate the contribution of the correction layers φ_{Θ_2} , we perform an ablation study using two baseline methods:

- **Rounding after Learning (RL):** This baseline trains only the first neural network π_{Θ_1} , which predicts relaxed solutions. Rounding to the nearest integer is applied post-training, meaning that the rounding step does not participate in the training process. This isolates the effect of excluding the corrective adjustments provided by φ_{Θ_2} . This baseline highlights the limitations of naively rounding relaxed predictions. Such rounding often leads to significant deviations in the objective value and feasibility violations, emphasizing the importance of end-to-end learning where updates are guided by the ultimate loss function.
- **Rounding with STE (RS):** In this baseline, continuous values predicted by π_{Θ_1} are rounded during training using the Straight-Through Estimator (STE), as shown in Algorithm 3. This approach allows gradients to flow through the rounding operator, facilitating optimization of the loss function even with integer constraints. This allows gradients to pass through the rounding operator, enabling optimization of the loss function in the presence of integer constraints. However, the rounding mechanism relies solely on fixed nearest-integer corrections, which are determined independently of the problem parameters or the relaxed predictions. Consequently, it lacks the refinement provided by learnable correction layers, limiting its ability to adjust the rounding to improve objective values and feasibility.

Algorithm 3 Rounding with STE: Forward Pass.

- 1: Training instance ξ^i and neural networks $\pi_{\Theta_1}(\cdot)$
 - 2: Predict a continuously relaxed solution $\bar{x}^i \leftarrow \pi_{\Theta_1}(\xi^i)$
 - 3: Round integer variables down: $\hat{x}_z^i \leftarrow \lfloor \bar{x}_z^i \rfloor$
 - 4: Compute \mathbf{b}^i as the rounding direction using Gumbel-Sigmoid($\bar{x}_z^i - \hat{x}_z^i - 0.5$)
 - 5: Update integer variables: $\hat{x}_z^i \leftarrow \hat{x}_z^i + \mathbf{b}^i$
 - 6: **Output:** \hat{x}^i
-

Results and Insights. The results of the ablation experiments, summarized in Table 8, Table 9 and Table 10, demonstrate the importance of the correction layers φ_{Θ_2} in improving both solution quality and feasibility. The experimental setup and model parameters used are consistent with those in the main text, ensuring the results are directly comparable. RL shows a significant drop in feasibility rates, highlighting the importance of incorporating differentiable rounding during training to guide outputs. Similarly, while RS benefits from differentiability via STE, the lack of learnable layers for rounding limits its performance compared to RC and LT.

F.2. Experiments with Varying Penalty Weights

To complement the findings in the main text, we extend our analysis to the 1000×1000 IQPs and the 2000×4 MIRBs. Figure 10 shows that these problems exhibit similar trends: higher penalty weights improve feasibility at the cost of increased

Table 8: Ablation Study for IQPs. See the caption of Table 2 for details.

Method	Metric	20×20	50×50	100×100	200×200	500×500	1000×1000
RL	Obj Mean	-4.726	-14.52	-17.22	-37.14	-89.81	-176.6
	Obj Median	-4.716	-14.52	-17.27	-37.15	-89.81	-176.6
	% Feasible	64%	42%	23%	10%	0%	0%
	Time (Sec)	0.0004	0.0004	0.0005	0.0005	0.0005	0.0011
RS	Obj Mean	-3.929	-11.93	-10.58	-24.72	-54.93	-110.7
	Obj Median	-3.963	-11.96	-10.58	-24.72	-54.93	-110.6
	% Feasible	100%	100%	100%	100%	100%	100%
	Time (Sec)	0.0010	0.0011	0.0013	0.0012	0.0016	0.0031

Table 9: Ablation Study for INPs. See the caption of Table 3 for details.

Method	Metric	20×20	50×50	100×100	200×200	500×500	1000×1000
RL	Obj Mean	-0.138	-0.629	-1.581	-4.196	-11.531	-23.64
	Obj Median	-0.148	-0.655	-1.554	-4.196	-11.531	-23.64
	% Feasible	87%	51%	15%	0%	0%	0%
	Time (Sec)	0.0005	0.0005	0.0006	0.0006	0.0006	0.0013
RS	Obj Mean	0.292	1.734	2.849	4.921	9.511	25.36
	Obj Median	0.284	1.736	2.841	4.907	9.511	25.36
	% Feasible	100%	100%	100%	100%	100%	100%
	Time (Sec)	0.0012	0.0011	0.0012	0.0013	0.0018	0.0031

Table 10: Ablation Study for MIRBs. See the caption of Table 4 for details.

Method	Metric	2×4	20×4	200×4	2000×4	20000×4
RL	Obj Mean	58.34	63.70	605.9	6222	68364
	Obj Median	58.00	61.95	609.0	5950	69087
	% Feasible	14%	64%	56%	72%	69%
	Time (Sec)	0.0006	0.0005	0.0005	0.0008	0.0014
RS	Obj Mean	25.095	69.36	684.7	6852	72910
	Obj Median	25.353	68.58	663.1	6509	68904
	% Feasible	100%	97%	100%	99%	61%
	Time (Sec)	0.0010	0.0010	0.0012	0.0019	0.0103

objective values, while feasibility projection effectively corrects solutions obtained with smaller penalty weights, preserving their lower objective values.

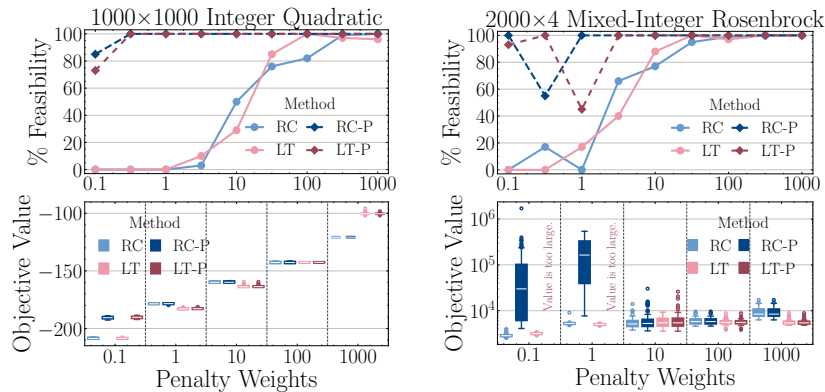


Figure 10: Illustration of the Proportion of feasible solutions (Top) and objective values (Bottom) for smaller-scale problems. For these instances, EX finds feasible solutions within 1000 seconds (leftmost values on the bottom), serving as a benchmark. Our approach, with properly tuned penalty weights, achieves comparable or even better objective values.

Additionally, we evaluate smaller-scale instances against exact solvers where exact solvers (EX) can find feasible solutions within the 1000-second time limit for all test instances. Figure 11 presents results for these instances, illustrating the proportion of feasible solutions and objective values across different penalty weights. These results further confirm that the appropriate choice of penalty weight, when combined with feasibility projection, can yield high-quality, feasible solutions. Thus, our method achieves comparable or even superior objective values to EX while solving instances orders of magnitude faster.

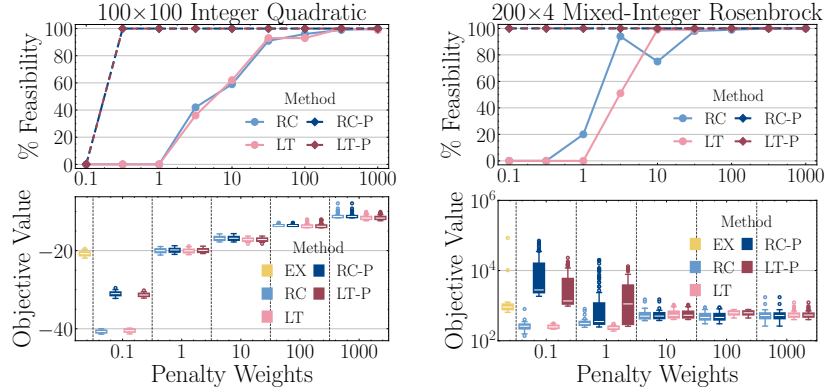


Figure 11: Illustration of the Proportion of feasible solutions (Top) and objective values (Bottom) for smaller problems. For these instances, EX can find feasible solutions within 1000 seconds (leftmost values on the bottom), serving as a benchmark. Our approach, with properly tuned penalty weights, achieves comparable or even better objective values.

F.3. Experiments with Varying Training Sample Size

To evaluate the effect of training sample size, we trained the model on datasets containing 800, 8,000, and 80,000 instances. Training epochs were adjusted to 2,000, 200, and 20 (with early stopping enabled) to ensure a comparable number of optimization iterations across experiments. All other hyperparameters were kept consistent to isolate the effect of sample size.

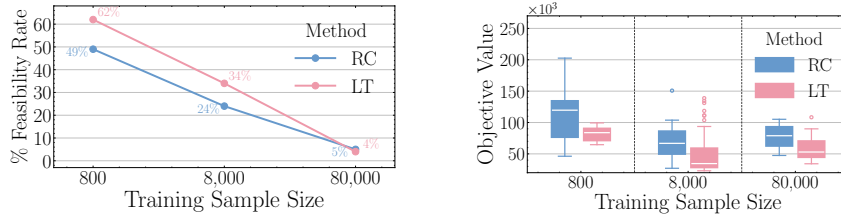


Figure 12: Illustration of the objective value (Left) and proportion of infeasible solutions (Right) of 20000x4 MIRBs on the test set. As the training sample size increases, the fraction of infeasible solutions decreases while the objective value generally deteriorates, as expected.

The result demonstrates that increasing the sample size yields significant improvements in both objective values and feasibility. For instance, training with 80,000 samples reduced the infeasibility rate to 5% on the test set, compared to much higher rates with smaller datasets. This emphasizes the critical role of sufficient sample size and demonstrates the scalability advantage of our self-supervised framework.

F.4. Experiments on Binary Linear Programs

Dataset. The ‘Obj Series 1’ dataset from the MIP Workshop 2023 Computational Competition (Bolusani et al., 2023) is conducted To evaluate the performance of our methods on MILPs. This dataset comprises 50 related MILP instances derived from a shared mathematical formulation. The instances differ in 120 of the 360 objective function coefficients, while all other components, including the constraints, remain consistent. Each instance includes 360 binary variables and 55 constraints, offering a structured benchmark for optimization methods.

Model Configuration. The neural network architecture and hyperparameters were consistent with those used in the main experiments. Specifically for the MILP problem in this study, the input dimension of the neural network was set to 120, corresponding to the number of varying objective function coefficients, and the output dimension was set to 360, representing the decision variables. The hidden layer consisted of 256 neurons.

Results. Table 11 summarizes the performance of various optimization methods on the MILP benchmark: Both learning-based methods (RC and LT) demonstrate the ability to generate high-quality feasible solutions efficiently, with RC even

Learning to Optimize for Mixed-Integer Nonlinear Programming

Table 11: Comparison of Optimization Methods on the MILP. See the caption of Table 2 for details.

Method	Obj Mean	Obj Median	% Feasible	Time (Sec)
RC	9745.90	9763.00	100%	0.04
LT	14149.00	14149.00	100%	0.04
EX	8756.80	8747.00	100%	28.91
N1	11901.10	11933.00	100%	0.01

surpassing the heuristic-based method N1 in terms of objective value. However, N1 is the fastest method overall, showcasing the robustness and efficiency of the heuristic in the MILP solver. EX achieved the best objective values but required significantly more computation time. Notably, the training time for the learning-based models is approximately 120 seconds, making them well-suited for applications requiring repeated problem-solving.